Development 138, 1675-1685 (2011) doi:10.1242/dev.060210

Role of epidermal primary cilia in the homeostasis of skin and hair follicles

Mandy J. Croyle[1,*], Jonathan M. Lehman[1,*], Amber K. O'Connor[1,*], Sunny Y. Wong[2], Erik B. Malarkey[1], Daniela Iribarne[2], William E. Dowdle[2], Trenton R. Schoeb[3], Zoe M. Verney[4], Mohammad Athar[4], Edward J. Michaud[5], Jeremy F. Reiter[2] and Bradley K. Yoder[1,†]

SUMMARY

Skin and hair follicle morphogenesis and homeostasis require the integration of multiple signaling pathways, including Hedgehog (Hh) and Wingless (Wnt), and oriented cell divisions, all of which have been associated with primary cilia. Although studies have shown that disrupting dermal cilia causes follicular arrest and attenuated Hh signaling, little is known about the role of epidermal cilia. Here, epidermal cilia function was analyzed using conditional alleles of the ciliogenic genes *Ift88* and *Kif3a*. At birth, epidermal cilia mutants appeared normal, but developed basaloid hyperplasia and ingrowths into the dermis of the ventrum with age. In addition, follicles in the tail were disorganized and had excess sebaceous gland lobules. Epidermal cilia mutants displayed fewer long-term label-retaining cells, suggesting altered stem cell homeostasis. Abnormal proliferation and differentiation were evident from lineage-tracing studies and showed an expansion of follicular cells into the interfollicular epidermis, as is seen during wound repair. These phenotypes were not associated with changes in canonical Wnt activity or oriented cell division. However, nuclear accumulation of the ΔNp63 transcription factor, which is involved in stratification, keratinocyte differentiation and wound repair, was increased, whereas the Hh pathway was repressed. Intriguingly, the phenotypes were not typical of those associated with loss of Hh signaling but exhibited similarities with those of mice in which ΔNp63 is overexpressed in the epidermis. Collectively, these data indicate that epidermal primary cilia may function in stress responses and epidermal homeostasis involving pathways other than those typically associated with primary cilia.

KEY WORDS: Cilia, Hair follicle, Epidermal homeostasis, Hyperplasia, Hedgehog, ΔNp63 (Trp63), Repair response, Mouse

INTRODUCTION

The skin performs its protective function by forming a stratified epithelium, the morphogenesis of which begins during embryogenesis when a single layer of ectoderm adopts an epidermal fate and differentiates into basal keratinocytes that express keratin 5 (K5, or Krt5) and K14 (for reviews, see Blanpain and Fuchs, 2006; Blanpain and Fuchs, 2009). Stratification of the epidermis initiates when basal keratinocytes give rise to suprabasal spinous keratinocytes that express K1 and K10. These cells further differentiate into the granular and cornified layers of the epidermis, eventually being shed into the environment and replaced by underlying cells. Thus, skin homeostasis is dependent on a balance between cell proliferation, differentiation and the shedding of cells ultimately derived from basal keratinocytes.

In the case of injury, follicular keratinocytes can exit the differentiation program and respond with increased proliferation and migration to repair the wound (Blanpain and Fuchs, 2009). The main sources of this regenerative capacity are progenitor/stem cells within the interfollicular basal layer and the follicle (for reviews, see Cotsarelis et al., 1990; Fuchs, 2009; Watt and Jensen, 2009), which are characterized by slow proliferation and long-term 5-bromo-2-deoxyuridine (BrdU) label retention (Cotsarelis et al., 1990; Morris and Potten, 1999; Tumbar et al., 2004).

Stratification of the epidermis is attained by self-renewing cells in the basal layer that each give rise to a clone of differentiating cells (Ito et al., 2005; Potten and Morris, 1988; Ro and Rannala, 2005). These clones consist of a few self-renewing progenitor cells in the basal layer together with the overlaying differentiated cells in the suprabasal layer. This stratification process in the skin requires the transcription factor Trp63 (p63) (Candi et al., 2006; Koster et al., 2004; Romano et al., 2007; Romano et al., 2009). p63 positively regulates expression of the basal keratinocyte markers K5 and K14. As such, mutations in *p63* result in a single-layered epidermis that lacks hair follicles (Mills et al., 1999), whereas overexpression of a p63 isoform (ΔNp63) in basal keratinocytes causes loss of canonical Wnt signaling, alopecia, and promotes interfollicular epidermal cell fates (Romano et al., 2010).

The formation of hair follicles relies on reciprocal interactions between cells in the epidermis and dermis and is mediated through multiple pathways [e.g. sonic hedgehog (Shh), Wnt] (for reviews, see Fuchs, 2007; Schneider et al., 2009). Briefly, around embryonic day (E)13, hair follicle formation is initiated by a dermal signal that induces the formation of a thickened region in the epidermis (placode), which then induces dermal cell aggregation (dermal condensate). The placode grows downwards, surrounding the dermal condensate, which becomes the dermal papilla. Continuous

[1]Department of Cell Biology, University of Alabama at Birmingham Medical School, Birmingham, AL 35294, USA. [2]Department of Biochemistry and Biophysics, Cardiovascular Research Institute, University of California, San Francisco, CA 94158, USA. [3]Department of Genetics, University of Alabama at Birmingham Medical School, Birmingham, AL 35294, USA. [4]Department of Dermatology Skin Disease Research Center, and UAB Comprehensive Cancer Center, University of Alabama at Birmingham Medical School, Birmingham, AL 35294, USA. [5]School of Physician Assistant Studies, South College, Knoxville, TN 37909, USA.

*These authors contributed equally to this work
†Author for correspondence (byoder@uab.edu)

Accepted 3 February 2011

reciprocal signaling between the epidermal and dermal cells regulates the downgrowth and differentiation of the multiple cell lineages of the adult pilosebaceous unit.

In adults, hair follicles undergo intermittent cycles of growth (anagen), apoptosis-mediated regression (catagen), and quiescence (telogen) (reviewed by Schneider et al., 2009). Follicle cycling involves many of the dermal and epidermal signaling pathways that function during morphogenesis. Lineage-tracing experiments indicate that the regenerative capacity of the follicle in adults is mediated by stem cells in the bulge located just beneath the sebaceous gland.

The Hedgehog (Hh) pathway has important roles in hair and skin development and maintenance. Shh is first expressed in the placode during initiation of follicle formation and again in a subpopulation of cells in the matrix of the mature follicle during the telogen to anagen transition. Mutations disrupting Shh or the downstream transcription factor Gli2 cause hair follicles to arrest during early morphogenesis (Gritli-Linde et al., 2007; Mill et al., 2003). This arrest is rescued in Gli2-deficient mice by transgenic expression of Gli2 in the basal cells using the *K5* promoter, suggesting that Hh signaling in the epidermal component of the follicle is sufficient for normal development (Allen et al., 2003; Gu and Coulombe, 2008; Mill et al., 2003).

The primary cilium has been implicated as a regulator of Hh signaling (Corbit et al., 2005; Gerdes et al., 2007; Huangfu et al., 2003; Haycraft et al., 2005) and in the control of the orientation of cell division (Fischer et al., 2006; Jonassen et al., 2008). Primary cilia are present on most cell types of the mammalian body and are maintained by intraflagellar transport (IFT). IFT mediates bidirectional movement of structural and signaling components between the base and tip of the cilium (reviewed by Goetz and Anderson, 2010), and mutations in genes such as *Ift88* and *Kif3a* disrupt IFT causing a wide variety of developmental and postnatal abnormalities (reviewed by Sharma et al., 2008).

The involvement of primary cilia in the processes utilized in hair and skin development raised the possibility that cilia might have an unappreciated role in the morphogenesis and homeostasis of the skin and skin diseases. We previously demonstrated that the ablation of cilia on dermal cells of the skin results in a phenotype that mimics the loss of Shh or Gli2, with an arrest of follicle development (Lehman et al., 2009). However, the role of epidermal cilia in skin and follicle morphogenesis and maintenance has not been explored. We address this here by examining mice in which the ciliogenic genes *Ift88* and *Kif3a* have been disrupted in the epidermis. Collectively, the results indicate that epidermal primary cilia are not essential for ventral or dorsal hair follicle morphogenesis. Intriguingly, the data suggest that cilia function in a pathway that is involved in epidermal stress responses, homeostasis of the interfollicular epidermis (IFE), and normal keratinocyte differentiation.

MATERIALS AND METHODS

Mice

The *Ift88* (*Ift88*^{tm1Bky}, hereafter *Ift88*^{F}) and *Kif3a* (*Kif3a*^{tm2Gsn}, hereafter *Kif3a*^{F}) conditional alleles were described previously (Haycraft et al., 2007; Marszalek et al., 2000). *Tg(KRT14-cre/ERT)20Efu* (*K14Cre*^{ERT}) mice were obtained from E. Fuchs (Vasioukhin et al., 1999). *K5-flx*^{GFPM2SMO} mice were obtained from Dr A. Dlugosz (Allen et al., 2003; Xie et al., 1998). *FVB-Tg(K14-Cre)8Brn* mice were obtained from Netherlands Cancer Institute (NCI), Amsterdam (Jonkers et al., 2001). *Tg(KRT14-cre)1Amc/J*, *Shh*$^{tm1(EGFP/cre)Cjt}$, *Gt(ROSA)26Sor*, *Gt(ROSA)26Sor*$^{tm4(ACTB-tdTomato,-EGFP)Luo}$ (mTmG) and *Ptch1*^{tm1Mps}*/J* (*Ptch1-lacZ*) mice were obtained from the Jackson Laboratory (Bar Harbor, ME, USA). Conditional cilia mutant mice were analyzed on a mixed C57BL/6J×129P2/OlaHsd genetic background. Mice were genotyped by PCR using tail or ear DNA (for primers, see Table S1 in the supplementary material). All animals were maintained in AAALAC accredited mouse facilities at UAB or UCSF and procedures were in accordance with the IACUC regulations of each institution.

Sample preparation, immunofluorescence and immunohistochemistry

Preparation of skin sections and immunofluorescence were conducted as described (Lehman et al., 2009). Whole-mount mouse tails were analyzed by immunofluorescence as described (Braun et al., 2003). Immunohistochemistry was performed using the Vectastain ABC Kit (Vector Laboratories, Burlingame, CA, USA) as per manufacturer's instructions. RNA was isolated using the RNeasy Kit (Qiagen, Valencia, CA, USA).

Antibodies used included anti-acetylated α-tubulin (Sigma, St Louis, MO, USA, T6793; 1:2000), anti-K5 (Covance, Berkeley, CA, USA, PRB-160P; 1:1000), anti-K1 (Covance, PRB-165P; 1:500), anti-NuMA (Novus Biologicals, NB500-174; 1:300), anti-laminin (Sigma, GW20044F; 1:200), anti-ΔNp63 (Santa Cruz, sc-8431; 1:50), anti-K17 (a gift of Dr Pierre Coulombe, John Hopkins University, Baltimore, MD, USA; 1:5000), anti-loricrin (Covance, PRB-145P; 1:500), anti-phosphohistone H3 (pH3) (Cell Signaling Technologies, Rab9763; 1:400), and anti-Arl13b (gift of Dr Caspary, Emory University, Atlanta, GA, USA; 1:2000). Nuclei were stained with Hoechst 33258 (Sigma).

Analysis of proliferation rates and long-term BrdU label retention

Proliferation was measured by BrdU injection as per the manufacturer's instructions [animal weight (g) × 30 μl; Invitrogen, Carlsbad, CA, USA) and skin isolated 2.5 hours post-injection. Long-term label retention was analyzed by injecting P10 mice with BrdU four times at 12-hour intervals.

Tail samples were taken 1, 19, 35 and 59 days post-injection and whole-mounts were prepared as above. Proliferation around the infundibulum of follicles was measured in *ShhCre* mutant and control mice at P23 by immunofluorescence analysis using anti-pH3. Four independent animals were analyzed per genotype (15 random follicles per animal).

β-galactosidase assays

For whole-mount analysis, skin biopsies were collected and fixed in 0.2% glutaraldehyde and 2% paraformaldehyde for 30 minutes on ice. After washing in *lacZ* buffer (2 mM $MgCl_2$, 0.01% NaDC, 0.02% NP40, in 100 mM sodium phosphate buffer, pH 7.3), tissues were incubated at 37°C in 1 mg/ml X-Gal diluted in 5 mM potassium ferrocyanide and 5 mM potassium ferricyanide (Taulman et al., 2001).

Cell clone size in cilia mutants

Clone size in *K14Cre*^{ERT}*;Kif3a*$^{F/Δ}$*;ROSA26* mice was determined from skin biopsies taken from three independent animals per genotype group at ~39 and 70 weeks after tamoxifen injection. For quantification, in each captured image the areas of the 20 most prominent β-galactosidase^{+} epidermal clones were measured using NIS-Elements software (AR 3.2, Nikon). A total of 120 clones were analyzed per genotype.

Analysis of the Hh pathway

The spatial activity of the Hh pathway was analyzed using the β-galactosidase assay with the *Ptch1-lacZ* reporter allele in P31 *K14Cre*^{AMC}*;Ift88*$^{F/F}$ mutant and control mice.

Hh pathway activity was determined by quantitative real-time (qRT) PCR analysis of RNA isolated from the tail epidermis using iQ SYBR Green Supermix (Bio-Rad, Hercules, CA, USA) with a CFX96 real-time PCR detection system (Bio-Rad). Primer sequences for qRT-PCR analysis of *Gli1*, *Ptch1*, *Ift88*, β-2 microglobulin (*B2m*) and *Gapdh* are listed in Table S1 in the supplementary material.

In situ hybridization

Formalin-fixed paraffin-embedded sections were used for in situ analysis as described (Grachtchouk et al., 2003). *Shh* probe was obtained from Dr A. P. McMahon (Harvard University, Cambridge, MA, USA). mRNA

expression was detected with anti-digoxygenin antibody conjugated to alkaline phosphatase (Roche Applied Science, Branchburg, NJ, USA) and visualized with BCIP/NBT chromogen solution (Roche Applied Science).

Orientation of cell divisions

Whole-mount tail preparations were probed with NuMA antibody as described (Braun et al., 2003). The spindle angle was calculated relative to the basement membrane using NuMA labeling in confocal image stacks (see Fig. S4 in the supplementary material for details). Analysis was performed using Volocity 5.3 software (PerkinElmer, Shelton, CT, USA) and Microsoft Excel 2007.

RESULTS

Spatial and temporal characterization of Cre expression and cilia loss

To begin addressing the functional importance of epidermal cilia, mice carrying the intraflagellar transport 88 (*Ift88*) conditional allele *Ift88*^{tm1bky} (hereafter *Ift88*^{F}) (Haycraft et al., 2007), or the kinesin family member 3A (*Kif3a*) conditional allele *Kif3a*^{tm2Gsn} (hereafter *Kif3a*^{F}) (Marszalek et al., 2000) were crossed with transgenic lines expressing Cre recombinase from a *K14* promoter (*K14Cre*). Two *K14Cre* lines with different temporal Cre activity were used. The *Tg(KRT14-cre)8Brn* line (hereafter *K14Cre*^{BRN}) (Jonkers et al., 2001) does not express Cre during development, has low mosaic Cre activity perinatally (see Fig. S1A in the supplementary material), but is expressed throughout the epidermis and follicle by postnatal day (P) 6, as determined using the Cre reporter line *Gt(ROSA)26S* (hereafter R26R). The *Tg(KRT14-cre)1Amc* (hereafter *K14Cre*^{AMC}) (Dassule et al., 2000) has higher and more uniform levels of Cre activity in the epidermal components of the skin and follicle as early as E12.5-13.5 (see Fig. S1B in the supplementary material), as determined using the Cre reporter line *Gt(ROSA)26Sor*$^{tm4(ACTB-tdTomato,-EGFP)Luo}$ (hereafter mTmG). In sections through the skin of *K14Cre*^{AMC} embryos at E14.5, Cre activity was uniform in the epidermis and absent in the dermis (see Fig. S1C in the supplementary material). At E16.5, Cre activity was evident throughout the developing follicle and interfollicular epidermis of the *K14Cre*^{AMC} embryos (see Fig. S1D in the supplementary material).

The presence or absence of cilia on the epidermis and hair follicle of adult *K14Cre* mutant and control mice was analyzed by immunofluorescence microscopy (see Fig. S2A,B in the supplementary material). In both *K14-cre*^{BRN}*;Ift88*$^{F/F}$ and *K14Cre*^{AMC}*;Ift88*$^{F/F}$ mutants, cilia were deleted from the cells in the epidermis of the follicle and in the interfollicular region (see Fig. S2A,C versus S2B,D in the supplementary material). Genotyping of DNA isolated from the epidermis or dermis of the tail of P31 *K14Cre*^{AMC}*;Ift88*$^{F/F}$ conditional mutants indicated a substantial decrease of the *Ift88* allele in the epidermis (see Fig. S2E in the supplementary material) as compared with the whole tail or dermis. The presence of a deleted allele in the dermis is likely to reflect contamination with epidermal cells. Western blot analysis of protein from the tail epidermis of the P31 *K14Cre*^{AMC}*;Ift88*$^{F/F}$ conditional mutant also showed near complete loss of Ift88 (see Fig. S2F in the supplementary material).

To evaluate Ift88 protein depletion, skin samples from E18.5 *K14Cre*^{AMC}*;Ift88*$^{F/F}$ mutant and control embryos were analyzed by immunofluorescence microscopy using antibodies against Ift88 and acetylated α-tubulin as a cilia marker. Although cilia could be detected in the epidermis of both *K14Cre*^{AMC}*;Ift88*$^{F/F}$ mutant and control embryos, in the conditional mutants these epidermal cilia did not contain Ift88, in contrast to dermal cilia (see Fig. S2G,H in the supplementary material). The persistence of cilia for a short period after inducing *Ift88* deletion is seen in vivo in the skin and kidney as well as in vitro using tamoxifen-inducible Cre *Ift88*$^{F/F}$ cell lines (B.K.Y., unpublished). Collectively, these data indicate that the *K14Cre*^{AMC} line disrupts IFT during development and would be useful for evaluating epidermal cilia function in hair follicle morphogenesis, whereas the *K14Cre*^{BRN} line would address the role of cilia in hair follicle cycling and epidermal homeostasis

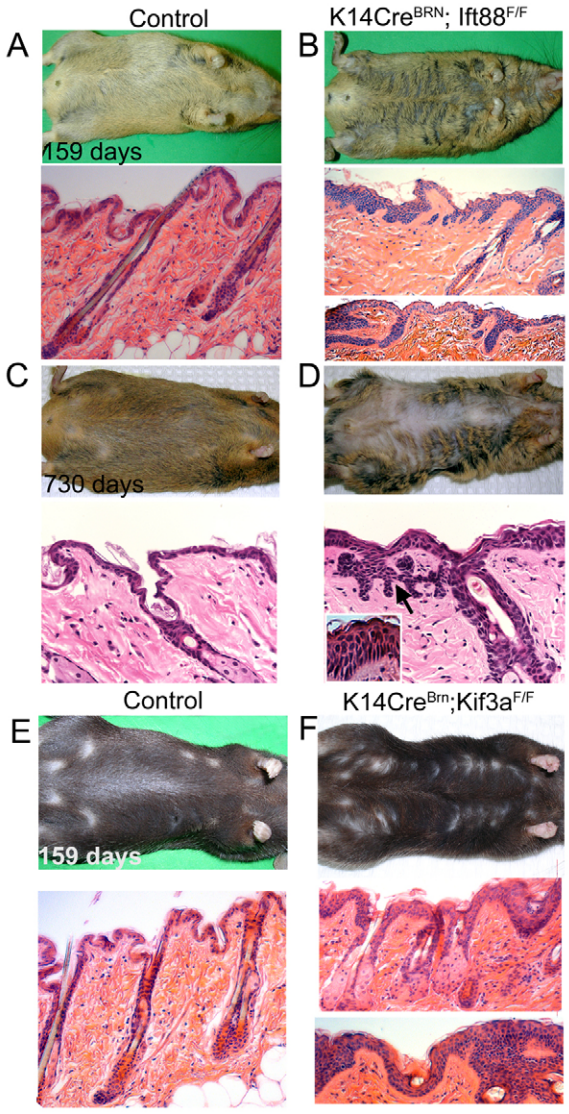

Fig. 1. Deletion of epidermal cilia causes ventral alopecia, basaloid hyperplasia, and epidermal ingrowths. (**A-F**) Gross appearance (top rows) and histological analysis (bottom rows) of the pelage and skin from control (A,C,E), *K14Cre*^{BRN}*;Ift88*$^{F/F}$ (B,D) and *K14Cre*^{BRN}*;Kif3a*$^{F/F}$ (F) conditional mutant mice. Compared with controls, *K14Cre*^{BRN}*;Ift88*$^{F/F}$ and *K14Cre*^{BRN}*;Kif3a*$^{F/F}$ mice have a ridged appearance to the ventral pelage with progressive alopecia from the age of 3 weeks. Images are from P159 (A,B,E,F) and P730 (C,D). Hematoxylin and Eosin staining of sections shows basaloid hyperplasia and the palisading morphology of the basal keratinocytes in the epidermis of mutants (D, bottom inset) as compared with the thin normal epidermis (C). In older mice (P730), the epidermis is markedly thickened and shows epidermal ingrowths into the dermis (D, arrow) that resemble aborted hair buds without evident dermal papillae or condensates.

in adults. However, the caveat of this analysis is that Ift88 loss in the *K14Cre*^{AMC} line was not necessarily complete at the onset of follicle morphogenesis.

Phenotype of mice lacking epidermal cilia

In newborn epidermal cilia mutants generated with either of the *K14Cre* lines, there were no defects evident in the skin or follicle (data not shown); however, mutants began to exhibit a ruffled hair pattern on the ventrum at ~3 weeks of age. The phenotype became more severe over time and led to regions of alopecia in older animals (Fig. 1D). Identical phenotypes were obtained using the *Kif3a*$^{F/F}$ or *Ift88*$^{F/F}$ lines and in most cases data are shown for *Ift88*$^{F/F}$ mice (Fig. 1).

Histological abnormalities in the ventral skin of mutants included a thickened epidermis and basaloid hyperplasia (Fig. 1B). The hyperplasia was confined to the basal layer of the epidermis and there were no signs of hyperkeratosis, suggesting a healthy stratum corneum. In aged *K14Cre*^{AMC}*;Ift88*$^{F/F}$ mutants (P730), the basal epidermis showed morphological signs of palisading (Fig. 1D, inset), which is also seen in disorders associated with increased Shh activity (Nieuwenhuis et al., 2007; Nieuwenhuis et al., 2006). There were also epidermal ingrowths into the dermis that resembled ectopic hair buds (Fig. 1D, arrow). No tumors or blistering were ever seen in mutant (*K14Cre*^{BRN}*;Ift88*$^{F/F}$) mice.

Although the phenotype in the ventral skin was the same in each of the *K14Cre* mutant lines, the tails of *K14Cre*^{AMC} cilia mutants alone showed significant pilosebaceous dysgenesis compared with controls (Fig. 2B). In control animals, the pilosebaceous units of the tail were in groups of three equally spaced follicles positioned in rows along the skin, with each follicle having two sebaceous gland lobules (Fig. 2C). In the *K14Cre*^{AMC}*;Ift88*$^{F/F}$ cilia mutants, the follicles were in abnormal clusters, had five or more sebaceous gland lobules and were often misoriented (Fig. 2D). The phenotype in the tail was evident by at least P3 (Fig. 2H), when follicle-like structures were often seen in a swirled pattern distinct from that of littermate control mice (Fig. 2G,I).

Disruption of cilia in the adult epidermis expands clone size in the interfollicular epidermis

To characterize the thickened epidermis, we crossed mice carrying the *Kif3a*^{F} and *Ift88*^{F} conditional alleles with *Tg(KRT14-cre/ERT)20Efu* (hereafter *K14Cre*^{ERT}) (Vasioukhin et al., 1999) and R26R mice. Cilia loss was induced on the basal cells at 4.5 weeks of age by tamoxifen injection. Clone size in cilia mutant and control samples was then analyzed at 39 (Fig. 3A,B) and 70 (Fig. 3C,D) weeks post-injection. Interestingly, mutant clones were markedly larger than those of control mice (Fig. 3E,F).

To assess whether the increased clone size was associated with proliferation, we injected BrdU into adult *K14-Cre*^{AMC}*;Ift88*$^{F/F}$ and control mice. BrdU incorporation into basal (K5; Fig. 4A,B) and spinous (K1; Fig. 4C,D) cells was quantified in three-dimensional stacks of the epidermis in whole-mount tail samples. All of the animals analyzed were 4 to 6 months old and comparisons were made only between littermates. The number of proliferating cells/μm^2 was significantly increased in the IFE of mutants compared with controls (Fig. 4E; Student's *t*-test, $P<0.01$; there was no change in cell size in the mutants compared with controls). A modest, but insignificant increase, was also observed in the follicles (Fig. 4E; Student's *t*-test, $P=0.23$).

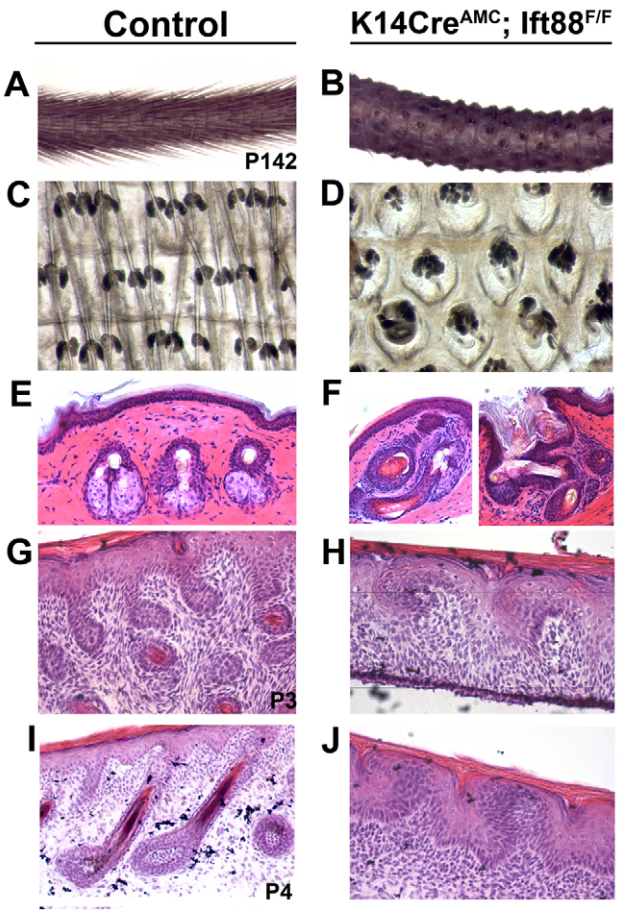

Fig. 2. The pilosebaceous units in the tail of *K14Cre*^{AMC}*;Ift88*$^{F/F}$ mutants are dysgenic. (**A-F**) The gross appearance of the tail phenotype of control (A) and *K14Cre*^{AMC}*;Ift88*$^{F/F}$ mutant (B) mice (P142). Mutants show severe dysgenesis of the hair follicle and skin. The pilosebaceous units in control mice (A,C,E) are regularly spaced, with three follicles in uniform groups, each having two sebaceous gland lobules. Follicles in *K14Cre*^{AMC}*;Ift88*$^{F/F}$ cilia mutants (B,D,F) are in abnormal clusters, each with five or more sebaceous gland lobules. The morphology of the hair shafts is curved rather than straight. A number of the follicles in the mutants (F, right) lack hair shafts and are dilated with keratinaceous debris. These phenotypes are not evident in the *K14-Cre*^{BRN}*;Ift88*$^{F/F}$ line (not shown), but they are fully penetrant in the *K14-Cre*^{AMC}*;Ift88*$^{F/F}$ mutants. (**G-J**) The phenotype in the tail can be detected at P3 (H) and P4 (J). Whereas follicles are clearly evident in the controls (G,I), they are poorly developed in the mutants (H,J), and those that are developing are disorganized.

Marker analysis of epidermal layers in cilia mutants

Markers for the different skin layers were used to characterize differentiation in the *K14Cre*^{Brn}*;Ift88*$^{F/F}$ line. Analysis of loricrin (Fig. 5A,B) and K1 (Fig. 5C,D) expression indicated that the granular and spinous layers are not hyperplastic. Expression of K1 (Fig. 5D) was discontinuous in the skin of conditional mutants, which was not evident in controls (Fig. 5C). By contrast, the K5 (Fig. 5F) basal layer was expanded in mutants compared with controls (Fig. 5E). Normally, K6 and K17 are expressed in sublayers of the hair follicle (Fig. 5G,I) (Gu and Coulombe, 2008; Panteleyev et al., 1997); however, in mutants, both K6 and K17 were detected ectopically in the IFE (Fig. 5H,J).

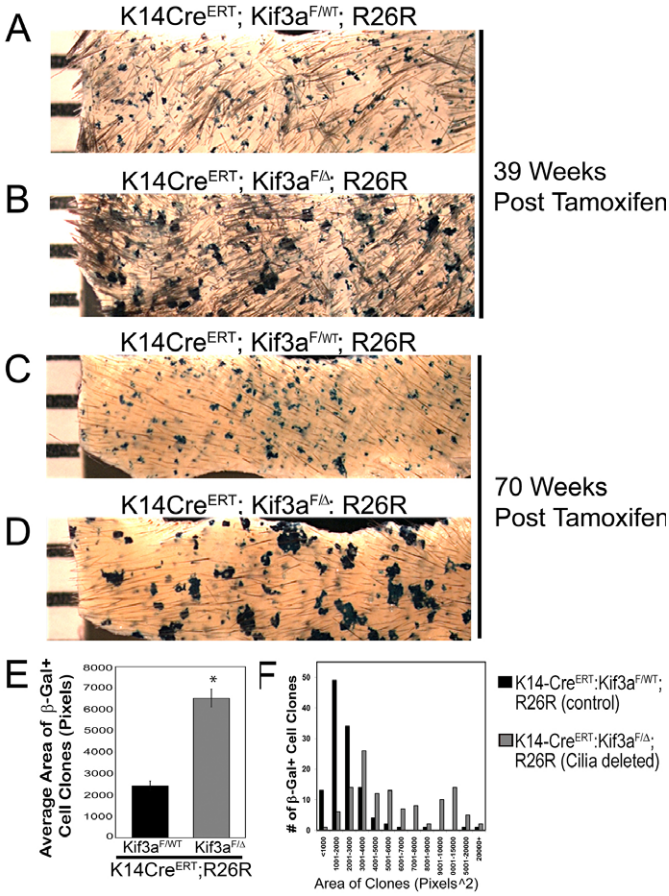

Fig. 3. Loss of epidermal cilia results in an expansion in clone size. (**A-D**) Clone size analyses were conducted in *K14Cre^{ERT};R26R;Kif3a$^{F/WT}$* (A,C) and *K14Cre^{ERT};R26R;Kif3a$^{F/Δ}$* (B,D) mutant mice by injection of 4.5-week-old mice with tamoxifen. Clonal expansion of cells in which Cre was activated (β-galactosidase positive, dark blue) was analyzed at 39 (A,B) and 70 (C,D) weeks post-injection. (**E**,**F**) There was a statistically significant increase (*, P<0.05) in the average size of the clones (E) and a change in the clone size distribution (F). Clone size (pixels^2) was determined using 120 clones for three independent animals for each genotype. Error bars indicate s.e.m.

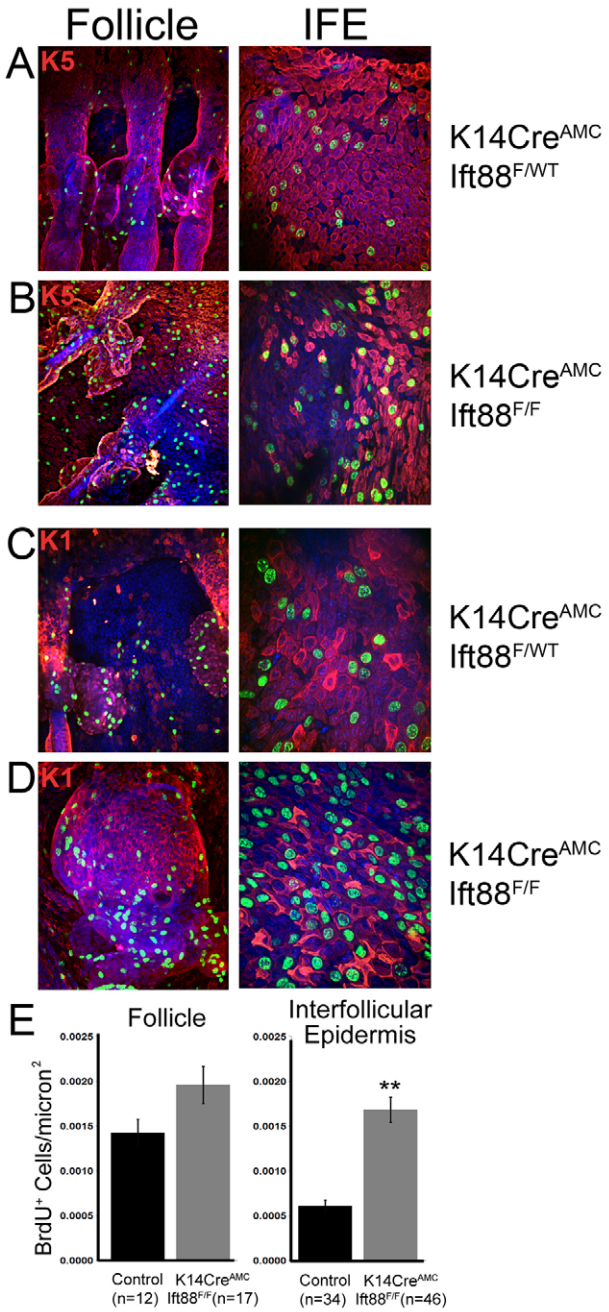

Fig. 4. Analysis of proliferation in epidermal cilia mutants. (**A-D**) Cell proliferation was analyzed by measuring the incorporation of BrdU (green) in adult *K14Cre^{AMC};Ift88$^{F/F}$* (B,D) and *K14Cre^{AMC};Ift88$^{F/WT}$* (A,C) mice after 2.5 hours. Increased proliferation was observed in mutants in both the basal (A,B; K5, red) and spinous (C,D; K1, red) layers of the follicle (left) and interfollicular epidermis (IFE) (right). Nuclei were stained with Hoechst (blue). (**E**) Quantification of proliferation as BrdU-positive cells/μm^2. Mice between 4 and 6 weeks of age were compared with sex-matched littermates. *, P<0.05; error bars indicate s.d.

Loss of epidermal cilia is associated with increased levels of ΔNp63

ΔNp63 is a transcriptional regulator that is normally expressed in basal keratinocytes of the proliferative layer and at a lower level in suprabasal differentiated layers of mature epidermis. It is required for commitment of the immature ectoderm to epidermal lineages, for epidermal maturation and maintaining the proliferative potential of basal keratinocytes, and its expression is induced by wounding (Koster et al., 2004; Mills et al., 1999; Romano et al., 2009; Romano et al., 2010; Yang et al., 1999); (Ichikawa et al., 2008). In addition, overexpression of ΔNp63 in the epidermis causes epidermal thickening, promotion of interfollicular epidermal fate and rapid depletion of follicular stem cells (Romano et al., 2009). Many of these phenotypes are seen in the epidermal cilia mutants (see below). In *K14Cre^{Amc};Ift88$^{F/F}$* mutants, there was a significant increase in ΔNp63 in the basal keratinocytes at P3 and P28 (Fig. 6A,C,D). ΔNp63 was also elevated in the K1 suprabasal layers of the P28 mutants (Fig. 6B), although this was not statistically significant (P=0.6). It is not yet known whether this effect on ΔNp63 is a direct or secondary consequence of cilia loss.

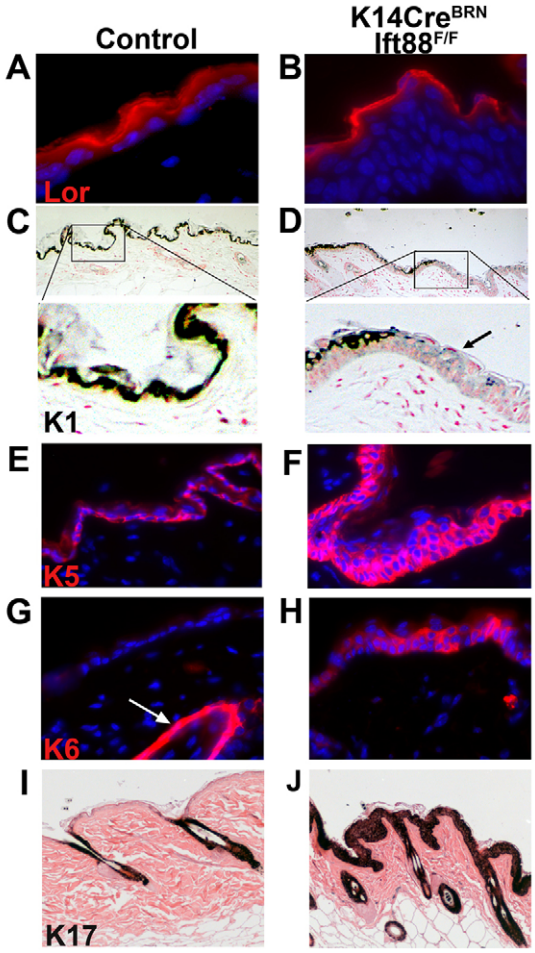

Fig. 5. Cell differentiation is abnormal in the epidermis of cilia mutants. (**A-J**) Sections of ventral epidermis were analyzed by immunofluorescence (A,B,E-H) or immunohistochemistry (C,D,I,J) for the expression of proteins in different cell layers of the epidermis from control (A,C,E,G,I) and *K14Cre^{BRN};Ift88$^{F/F}$* mutant (B,D,F,H,J) mice. There were no differences between mutant and control in the granular layer (A,B; anti-loricrin, red). In control mice (C), the spinous layer expresses K1 (black) in a single continuous layer, whereas in mutant mice K1 is discontinuous (D; arrow). The basal layer of mutants (F) was markedly expanded compared with that of controls (E), as shown by K5 staining (red). Mutants (H) also showed ectopic expression of the companion cell layer marker K6 (red) compared with controls (G; arrow indicates K6 expression in the follicle). K17 (brown), which is expressed in the outer root sheath as well as in other follicle subdomains, was ectopically expressed in the IFE of the mutant (J) as compared with controls (I).

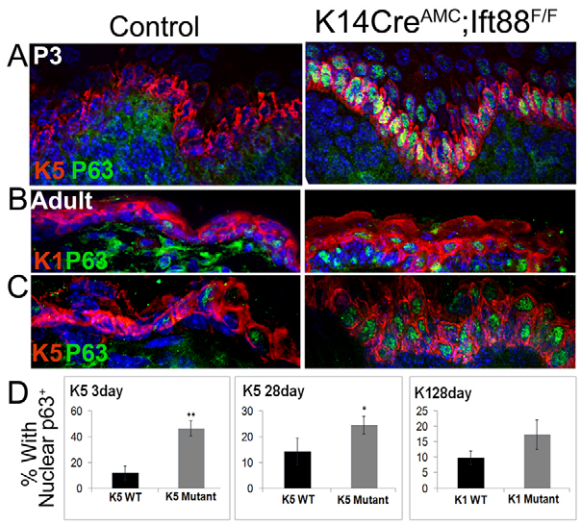

Fig. 6. Analysis of ΔNp63 expression in epidermal cilia mutants. (**A-C**) Analysis of ΔNp63 (green) expression in spinous (B; K1, red) and basal cell (A,C; K5, red) layers of P3 (A) and P28 (B,C) control (left) and *K14Cre^{AMC};Ift88$^{F/F}$* mutant (right) mice. (**D**) Quantification of the levels of ΔNp63 in *K14Cre^{AMC};Ift88$^{F/F}$* and control samples. *, $P<0.05$; **, $P<0.01$; error bars indicate s.e.m.

Comparison of epidermal cilia mutants with mice with epidermal activated Hh

The phenotypes of the epidermal cilia mutants are reminiscent of those of mice with a truncated form of the Shh receptor patched 1 (Ptch1) (Nieuwenhuis et al., 2007) and of mice in which the Shh pathway is ectopically activated in basal cells (Adolphe et al., 2004). These shared phenotypes, along with the connection between Hh and cilia, prompted a comparison between the epidermal cilia mutants and mice expressing activated smoothened (Grachtchouk et al., 2003; Wong et al., 2009). To accomplish this, we generated *K14Cre^{BRN};K5-M2SMO* (*K5-flxGFP-M2SMO*) (Xie et al., 1998) mice in which Cre-mediated excision of a stop sequence between the *K5* promoter and a *M2SMO* (activated) minigene induces expression of smoothened in the basal cells. Both the *K5-M2SMO* and cilia mutant mice had a 'scruffy' ventral appearance, an expanded basal layer, ectopic epidermal ingrowths (Fig. 7B,C, arrows) (Hoseong Yang et al., 2008) and ectopically expressed K17 (Fig. 5J and see Fig. S3 in the supplementary material). Generally, the phenotype of the epidermal cilia mutants was less severe than that of the activated smoothened mice.

Elevated Hh activity might occur in epidermal cilia mutants as a consequence of the requirement for cilia in Gli repressor formation (Haycraft et al., 2005; Huangfu and Anderson, 2005; Huangfu et al., 2003; Liu et al., 2005). Alternatively, repression of the Hh pathway could also be responsible as cilia are required for the activation of Gli (Haycraft et al., 2005; Huangfu et al., 2003). To distinguish between these scenarios, expression of the Hh target genes *Gli1* and *Ptch1* was examined by qRT-PCR in RNA isolated from tail epidermis of P31 *K14Cre^{AMC};Ift88$^{F/F}$* mice (Fig. 7D). Expression of both *Gli1* and *Ptch1* was decreased along with that of *Ift88* in the mutants. The spatial activity of the Hh pathway was analyzed in the skin of P31 *K14Cre^{AMC};Ift88$^{F/F}$* mutant and control mice using the *Ptch1-lacZ* reporter line. Similar to the qRT-PCR data, the Hh pathway was found to be repressed in the follicles of cilia mutants as compared with controls (Fig. 7E). There was no pathway activity evident in the IFE of either mutant or controls (data not shown).

Loss of cilia on cells that express *ShhCre* results in an expansion of follicular cells into the IFE

To more specifically analyze primary cilia in the hair follicle, we crossed the *Ift88$^{F/F}$* and *Kif3a$^{F/F}$* mice onto the *Shh$^{tm1(EGFP/cre)Cjt}$* (hereafter *ShhCre*) (Harfe et al., 2004; Levy et al., 2005). *ShhCre* is expressed in the placode during morphogenesis and in the lateral disc of matrix cells in anagen follicles (Levy et al., 2005). Descendants of *ShhCre*-expressing cells contribute only to the follicle during

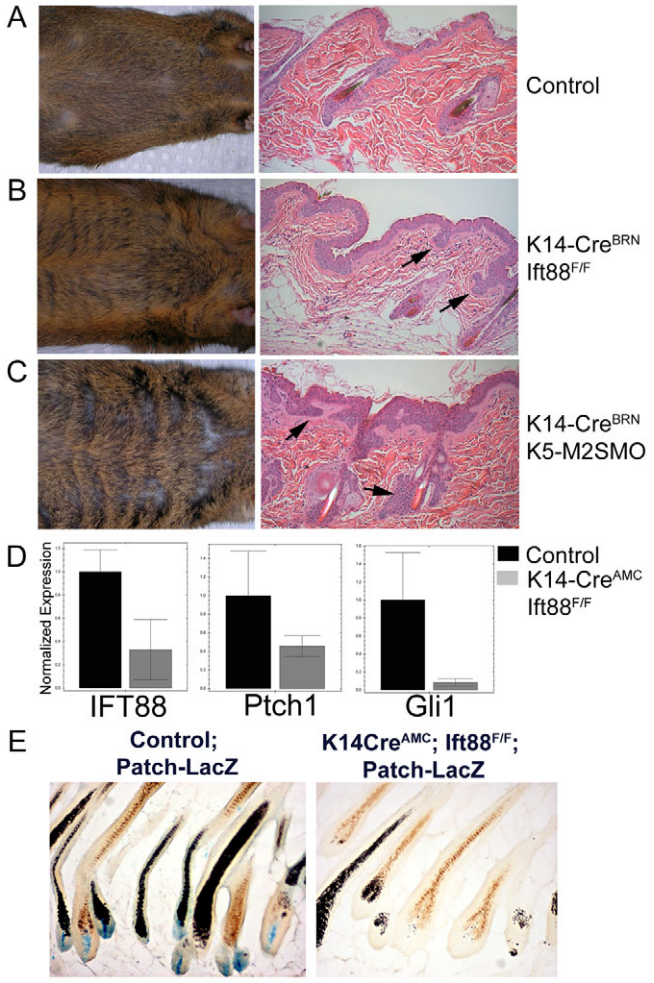

Fig. 7. Comparison of epidermal cilia mutant phenotypes with those of mice expressing an activated form of smoothened in the basal layer. (**A-C**) Gross appearance (left) and histological analysis (right) of the pelage and skin from control (A), *K14Cre*^{BRN}*;Ift88*$^{F/F}$ (B) and *K14Cre*^{BRN}*;K5-M2SMO* (C) mice. A similar, but milder phenotype, is observed in epidermal cilia mutants (B) as compared with mice expressing activated smoothened in epidermal basal cells (C). Specifically, ventral ridging, a thickened epidermis and aborted follicles are observed. Arrows (B,C) indicate hair bud-like ingrowths. (**D**) Quantitative RT-PCR analysis shows that *Ift88*, as well as *Ptch1* and *Gli1*, are markedly reduced in RNA isolated from tail epidermis of P31 *K14Cre*^{AMC}*;Ift88*$^{F/F}$ mutants relative to controls. Error bars indicate s.e.m. (**E**) Spatial activity of the Hh pathway was evaluated in P31 *Ift88*$^{F/F}$*;Ptch1-lacZ* control (left) and *K14Cre*^{AMC}*;Ift88*$^{F/F}$*;Ptch1-lacZ* (right) mice.

development. Similar to the results obtained in the *K14Cre* mutants, *ShhCre* cilia mutants did not exhibit defects in hair follicle development, despite the follicles being largely composed of descendants from Cre-expressing cells (Fig. 8B). In part, this might reflect stability of the cilium after *Ift88* or *Kif3a* has been deleted, although most cells that expressed Cre did not have primary cilia, and those that were retained were severely truncated (Fig. 8C). To conduct lineage-tracing studies we crossed the *ShhCre* mice onto the R26R line and found that the mutants showed that the cells in which Cre had been expressed were markedly expanded (Fig. 8D) and were present abnormally in the IFE (Fig. 8B,E,F, arrows).

The presence of follicular cells in the IFE normally occurs only in response to wounding (Ito et al., 2005; Levy et al., 2005; Levy et al., 2007). In situ analysis showed that *Shh* is expressed normally in the lateral disc within the matrix cells (Fig. 8G) (St-Jacques et al., 1998) and not in the IFE. Thus, the ectopic cells in the IFE are likely to result from the migration of follicular cells into the IFE and not from ectopic *Shh* expression (Fig. 8B,D-F). Furthermore, in *ShhCre* cilia mutants, there was ectopic expression of K17 (Fig. 8H) and increased ΔNp63 (Fig. 8H, left) in these clones. This was similar to what was seen in the IFE of *K14Cre* cilia mutants (Fig. 5J), although we did not observe a population that co-expressed K6 (Fig. 8H, right).

Analysis of the IFE and hair follicle progenitor/stem cells in epidermal cilia mutants

The expanded K5-positive basal cell layer, altered keratinocyte differentiation and the epidermal thickening suggested that the phenotype might be associated with an abnormal maintenance of progenitor cell populations. This was analyzed using long-term label-retention assays (Cotsarelis et al., 1990; Morris and Potten, 1999; Tumbar et al., 2004). In the hair follicle, retention of BrdU label after a long chase period is used as an indicator of progenitor cells. For this analysis, P10 control and epidermal cilia mutant mice (*K14Cre*^{AMC}*;Ift88*$^{F/F}$) were injected with BrdU four times over a 48-hour period, which labels most cells in the follicle and IFE (Fig. 9A,B, insets). The depletion of label, relative to the day after BrdU injection, was evaluated in whole-mount tail epidermis 19, 35 and 59 days post-injection. The number of cells retaining label after each chase period was not markedly different in the IFE of mutants and controls (Fig. 9C,D). By contrast, in the follicle there was a greater and more rapid decrease in the number of cells retaining label in the mutants compared with controls. This was especially evident at day 19 (16.3% in controls versus 5.8% in mutants; Student's *t*-test, $P<0.05$; Fig. 9A,B,E). At the end of the chase period there were fewer labeled cells in the bulge region of mutants, with many follicles lacking labeled cells (Fig. 9B,D).

The axis of cell division is unaffected in cilia mutants

In the kidney, ciliary dysfunction can cause the misorientation of cell divisions (Fischer et al., 2006; Jonassen et al., 2008; Patel et al., 2008). The expansion of the basal layer in the epidermal cilia mutants raised the possibility that altered cell divisions might contribute to the phenotypes. This possibility was evaluated in whole-mount tail preparations from control and *K14Cre*^{AMC}*;Ift88*$^{F/F}$ adult mice by staining with antibodies against nuclear mitotic apparatus protein (NuMA; Numa1 – Mouse Genome Informatics) (see Fig. S4 in the supplementary material) (Lechler and Fuchs, 2005). The angle of the spindle was measured relative to the plane of the basal membrane. There were no significant differences in either the IFE or follicles of mutants versus controls in the distribution of the angles of cell division (Student's *t*-test; follicle, $P=0.97$; IFE, $P=0.72$), which were typically within 25 degrees of the basal membrane (see Fig. S4 in the supplementary material).

DISCUSSION

Primary cilia are present on most cell types in the skin (Elofsson et al., 1984; Lehman et al., 2009; Lehman et al., 2008; Wandel et al., 1984; Warfvinge and Elofsson, 1988), yet their functional importance in the morphogenesis and maintenance of the skin and follicle is only now being investigated. Loss of dermal cilia results in follicular arrest due to attenuated Hh signaling (Lehman et al.,

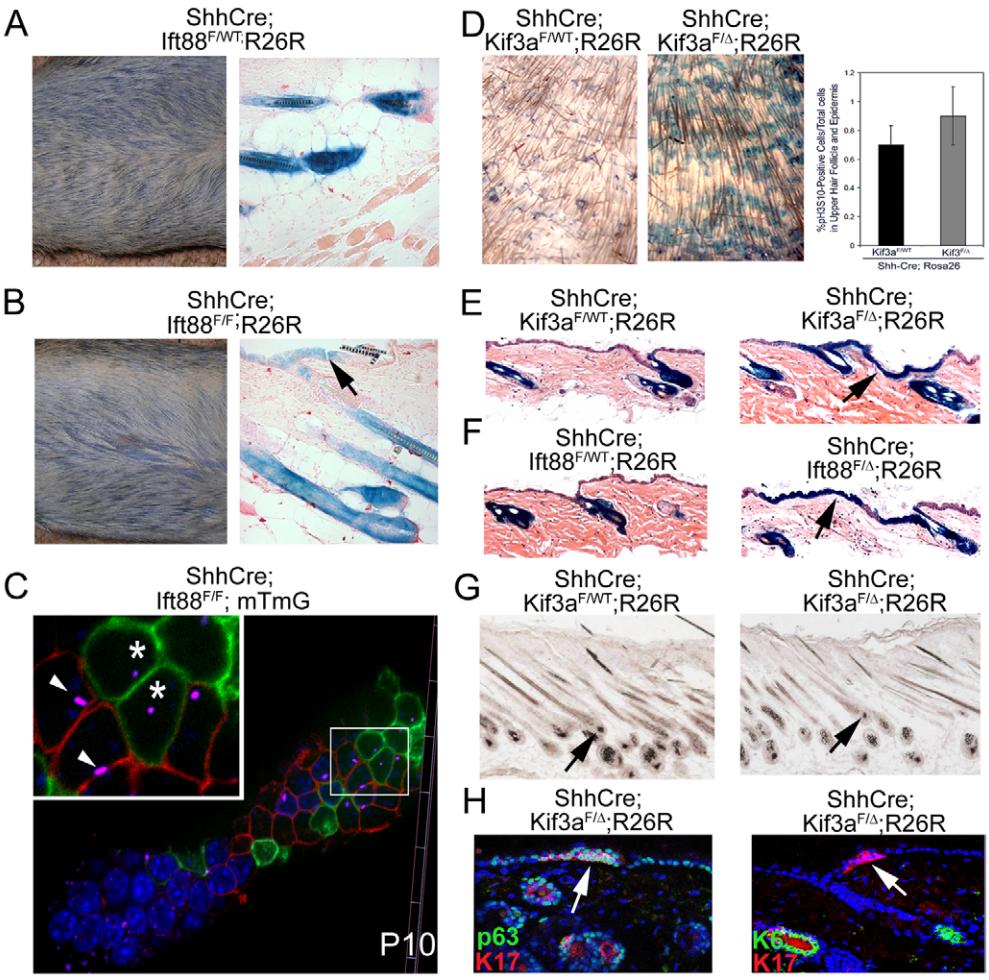

Fig. 8. Disruption of cilia on Shh-expressing cells does not disrupt morphogenesis but does cause expansion of follicular cells into the IFE. (**A**,**B**) The pelage (left) of control (A) and *ShhCre;Ift88*$^{F/F}$ (B) mice show no overt differences. Analysis of Cre activity (right) with R26R in control (A) and conditional mutant (B) mice shows strong β-galactosidase activity in most follicles of both genotypes. Arrow (B) indicates ectopic follicular cells in the IFE. (**C**) Cilia loss was analyzed by immunofluorescence in P10 *ShhCre;Ift88*$^{F/F}$ mice on the mTmG reporter background using antibodies against the ciliary protein Arl13b (purple). The inset shows that Cre-positive cells in the follicle (green) have shortened cilia (purple, asterisks) compared with Cre-negative cells in the follicle (red), which have normal cilia (purple, arrowheads). Nuclei were stained with Hoechst (blue). (**D**) Comparison of β-galactosidase staining in 8-week-old *ShhCre;Kif3a*$^{F/WT}$*;R26R* control (left) and *ShhCre;Kif3a*$^{F/\Delta}$*;R26R* mutant (middle) mice shows that descendants of Shh-expressing cells (blue) extend from the infundibulum in mutants in contrast to controls. Cellular proliferation in P23 *ShhCre;Kif3a*$^{F/\Delta}$ and control mice (right) was analyzed in the infundibulum plus ten cells of the IFE on either side of the follicle by pH3 staining. A slight, but insignificant, increase in proliferation was seen *ShhCre;Kif3a*$^{F/\Delta}$ mutants compared with controls (P=0.43; error bars indicate s.e.). (**E**,**F**) Cilia mutant cells (*ShhCre;Kif3a*$^{F/\Delta}$ or *ShhCre;Ift88*$^{F/\Delta}$) generated with *ShhCre* localize aberrantly in the IFE (arrows; see also B). (**G**) The cells that expand into the IFE region of *ShhCre;Kif3a*$^{F/\Delta}$*;R26R* mice do not actively express *Shh*, which is only seen in the lateral disc (arrows) of the matrix cells as shown by in situ hybridization. (**H**) The expanding cells from the infundibulum of the follicle of *ShhCre;Kif3a*$^{F/\Delta}$ mice ectopically co-express K17 (red) and ΔNp63 (green) (left, arrow). Ectopic cells expressing K17 (right, arrow) did not co-express K6 in *ShhCre;Kif3a*$^{F/\Delta}$ mice.

2009). Here, we demonstrate that the loss of cilia on the epidermis has a minimal or no effect on morphogenesis of the ventral and dorsal hair follicles, but has a marked impact on skin homeostasis. For example, we observed progressive epidermal ridging, ventral alopecia, basaloid hyperplasia, abnormal keratinocyte differentiation and ectopic epidermal ingrowths into the dermis. In the tail of the early cilia mutant line (*K14Cre*$^{\Delta MC}$), the phenotype is more severe: the follicles are dysmorphic, abnormally clustered and possess excess sebaceous gland lobules, demonstrating that cilia are required for tail follicle morphogenesis.

The minimal follicular phenotype is an intriguing finding considering the known importance of Hh in hair follicle morphogenesis and cycling (Corbit et al., 2005; Gritli-Linde et al., 2007; Haycraft et al., 2005; Liu et al., 2005; May et al., 2005; St-Jacques et al., 1998). The alopecia in *Gli2* mutant skin can be rescued by expressing Gli2 specifically in the K5-positive basal cells, further suggesting that Shh activity in the epidermis is crucial for normal follicle development (Mill et al., 2003). However, we find that phenotypes associated with the loss of Hh signaling are not evident in the epidermal cilia mutants, suggesting that Hh signaling through epidermal cilia is not required for follicle morphogenesis and cycling. Indeed, our data indicate that the pathway is attenuated in the epidermis. However, it remains possible that a sufficient number of cells with cilia might remain in the epidermis to allow normal development and cycling to proceed.

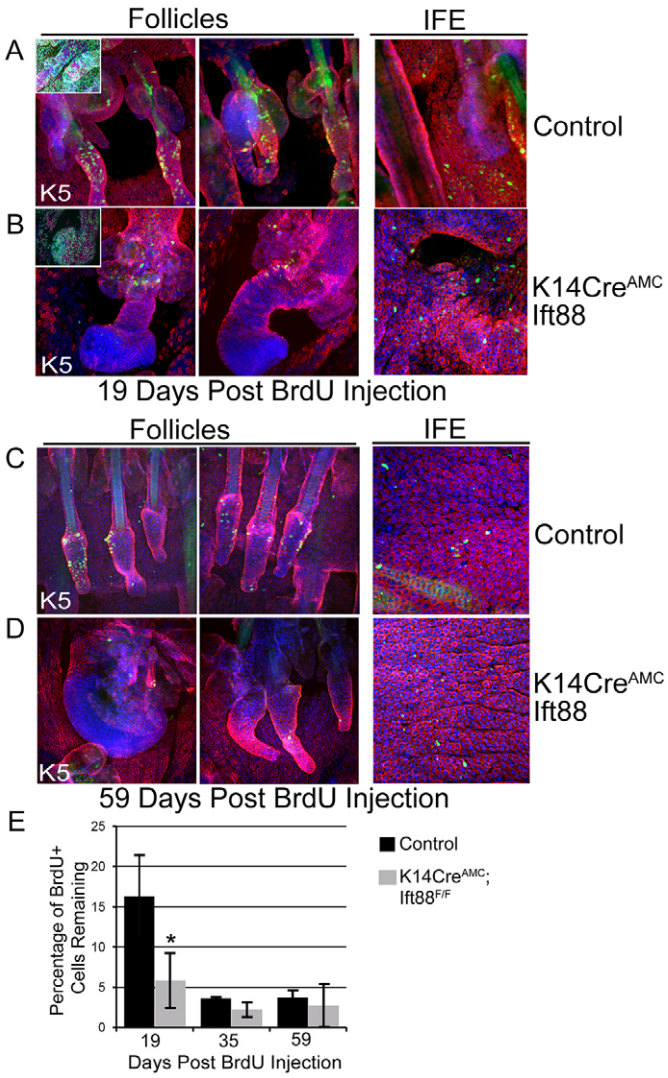

Fig. 9. Analysis of BrdU label retention in epidermal cilia mutants. (**A-D**) P10 control (A,C) and *K14Cre^{AMC};Ift88$^{F/F}$* (B,D) mutant mice were injected with BrdU four times over a 48-hour period. Depletion of label in the follicle or IFE of the tail was analyzed over a 19 (A,B) or 59 (C,D) day period following labeling. (**E**) Label retention was determined relative to that 24 hours after the last injection (as shown in A,B, insets). After 19 days, the mutants had a greater percentage reduction in the number of cells with label relative to the controls, particularly in the follicle. Similar results were seen after 35 and 59 days. *, $P<0.05$ for mutant versus control by Student's *t*-test; error bars indicate s.d. There were no significant differences between mutant and control in the number of label-retaining cells in the IFE. The basal cells were identified with anti-K5 (red).

In adults, two-thirds of the follicle is replenished each cycle largely from stem cells in the bulge (for reviews, see Blanpain and Fuchs, 2006; Blanpain and Fuchs, 2009; Fuchs, 2009). Intriguingly, epidermal cilia mutants have a marked reduction in the number of cells retaining BrdU label, suggesting a more rapid turnover of the stem cell population (Cotsarelis et al., 1990; Morris and Potten, 1999; Tumbar et al., 2004). This reduction implies that cilia have a role in stem cell homeostasis and helps explain the mild alopecia that is observed in older mutants.

In the *K14Cre* epidermal cilia mutants there is an increase in the number of cells expressing ΔNp63, particularly in the perinatal period. Increased ΔNp63, along with ectopic K17 expression, was observed in patches of cells located just outside of the follicles of the cilia mutants generated using *ShhCre*. Recently, a mouse expressing ΔNp63 in the epidermal basal layer was generated (Romano et al., 2010) and exhibits phenotypic overlap with the epidermal cilia mutant mice. For example, in both lines the expression of several keratins (K5, K17 and K6) was expanded and there was a reduction in the number of progenitor cells within the bulge. ΔNp63 is thought to promote interfollicular epidermal cell fates and our analysis in *ShhCre* lines suggests that a similar effect might be occurring in these mutants. However, there are also several key differences between the epidermal cilia mutants and the ΔNp63-overexpressing line. The cilia mutants do not show changes in terminally differentiated keratinocytes (loricrin staining), nor was there a decrease in proliferation within any domain of the follicular unit. Finally, the phenotypes of the ΔNp63-overexpressing mice were a consequence of reduced Wnt signaling, which was not evident in the epidermal cilia mutants (data not shown). Collectively, this indicates that although the activity of ΔNp63 is altered by the loss of cilia, this is not solely responsible for the phenotypes.

One theory concerning the regulation of differentiation and homeostasis in stem cell populations relies on control of the axis of division of basal keratinocytes (Lechler and Fuchs, 2005). Symmetric division parallel to the basement membrane is thought to result in two equivalent cells that replenish the basal stem cell population. By contrast, in an asymmetric division, the newly formed daughter cell is positioned into the suprabasal layer, initiating the differentiation program (Lechler and Fuchs, 2005). Thus, defects in the regulation of this process could cause an expansion of the basal population, as observed in the epidermal mutants. Furthermore, a precedent connecting cilia and the regulation of the orientation of cell division already exists in the kidney (Fischer et al., 2006; Jonassen et al., 2008; Patel et al., 2008). However, our analysis suggests that there were no differences between epidermal cilia mutants and controls with regard to their axis of division.

Lineage-tracing studies using a tamoxifen-inducible *K14Cre^{ERT}* line revealed that loss of cilia leads to an increase in clone size in adults. These clones ectopically express K17, suggesting that ciliary functions are involved in cell differentiation decisions or cell behavior, such as the migration of follicular cells into the IFE. This is further supported by the results from the *ShhCre* line that disrupts cilia only in the follicle, yet labels cells located in the mutant IFE. These ectopically positioned cells also express K17 and show elevated ΔNp63. Descendants of the Shh-expressing cells are normally restricted to the follicle but can contribute to the IFE under conditions of wounding (Levy et al., 2007). Based on these data and the depletion of label-retaining cells in the follicle, we propose that the loss of cilia on the epidermis might mimic conditions of epidermal damage or affects pathways involved in regulating a response to epidermal stress.

An association between the injury response and cilia has been noted previously. Primary cilia are temporarily elongated after obstruction of the pancreatic duct as well as after ureteral obstruction or ischemic reperfusion injury in the kidney (Hamamoto et al., 2002; Hellman et al., 2010; Verghese et al., 2009; Verghese et al., 2008; Wang et al., 2008). In addition, recent studies in the kidney have revealed that cyst development associated with cilia dysfunction is highly dependent on when cilia

loss occurs (Davenport et al., 2007; Piontek et al., 2007). In adult induced cilia mutants, renal cyst development is greatly enhanced by a subsequent injury. Together, these data support the idea that in the absence of the cilium, there is an inappropriate activation or impaired deactivation of a wound response that contributes to the pathogenesis. In the skin, this might cause inappropriate recruitment of cells out of the follicle into the interfollicular epidermis leading to epidermal thickening, ectopic expression of K17 and ΔNp63 and a more rapid turnover of the stem cell population.

In summary, these data indicate that cilia on epidermal cells are not essential for ventral or dorsal follicle morphogenesis, but are required for normal homeostasis of the IFE, normal label retention in the bulge and are possibly involved in regulating the stress response. Loss of epidermal cilia caused hyperplasia, increased ΔNp63, expanded clone size and altered keratinocyte differentiation. There were also changes in cell behavior, such that cells that should have been restricted to the follicle were present in the IFE and expressed ectopic keratins and other markers associated with a wound response. The phenotypes were not correlated with an alteration in the orientation of cell division or Wnt pathway activity; however, Shh signaling was attenuated. Interestingly, no Hh-related phenotypes were noted, suggesting that the epidermis is not the primary Hh-responsive component of the skin. Importantly, these data indicate that the function of primary cilia on epidermal cells is distinct from that on dermal cells and that the phenotype of the epidermal cilia mutants might involve novel pathways not previously associated with the cilium.

Acknowledgements

We thank the UAB Comparative Pathology Core for histology services; Pierre Coulombe and Michael Ruppert for K17 antibodies; Tamara Caspary for the Arl13b antibody; and Andrezj Dlugosz for the *K5-flx*^{GFPM2SMO} mice. This work was supported by a T32 predoctoral award (AR047512-07, Dr McDonald) to A.K.O.; postdoctoral fellowships from the American Cancer Society and the NIH (1K99AR059796) to S.Y.W.; by NIH RO1s (AR052792 and HD056030) to B.K.Y.; ES015323 to M.A.; and AR054396, March of Dimes, Burroughs Wellcome Fund, Packard Foundation and the Sandler Family Supporting Foundation to J.F.R. Deposited in PMC for release after 12 months.

Competing interests statement

The authors declare no competing financial interests.

Supplementary material

Supplementary material for this article is available at
http://dev.biologists.org/lookup/suppl/doi:10.1242/dev.060210/-/DC1

References

Adolphe, C., Narang, M., Ellis, T., Wicking, C., Kaur, P. and Wainwright, B. (2004). An in vivo comparative study of sonic, desert and Indian hedgehog reveals that hedgehog pathway activity regulates epidermal stem cell homeostasis. *Development* **131**, 5009-5019.

Allen, M., Grachtchouk, M., Sheng, H., Grachtchouk, V., Wang, A., Wei, L., Liu, J., Ramirez, A., Metzger, D., Chambon, P. et al. (2003). Hedgehog signaling regulates sebaceous gland development. *Am. J. Pathol.* **163**, 2173-2178.

Blanpain, C. and Fuchs, E. (2006). Epidermal stem cells of the skin. *Annu. Rev. Cell Dev. Biol.* **22**, 339-373.

Blanpain, C. and Fuchs, E. (2009). Epidermal homeostasis: a balancing act of stem cells in the skin. *Nat. Rev. Mol. Cell Biol.* **10**, 207-217.

Braun, K. M., Niemann, C., Jensen, U. B., Sundberg, J. P., Silva-Vargas, V. and Watt, F. M. (2003). Manipulation of stem cell proliferation and lineage commitment: visualisation of label-retaining cells in wholemounts of mouse epidermis. *Development* **130**, 5241-5255.

Candi, E., Rufini, A., Terrinoni, A., Dinsdale, D., Ranalli, M., Paradisi, A., De Laurenzi, V., Spagnoli, L. G., Catani, M. V., Ramadan, S. et al. (2006). Differential roles of p63 isoforms in epidermal development: selective genetic complementation in p63 null mice. *Cell Death Differ.* **13**, 1037-1047.

Corbit, K. C., Aanstad, P., Singla, V., Norman, A. R., Stainier, D. Y. and Reiter, J. F. (2005). Vertebrate Smoothened functions at the primary cilium. *Nature* **437**, 1018-1021.

Cotsarelis, G., Sun, T. T. and Lavker, R. M. (1990). Label-retaining cells reside in the bulge area of pilosebaceous unit: implications for follicular stem cells, hair cycle, and skin carcinogenesis. *Cell* **61**, 1329-1337.

Dassule, H. R., Lewis, P., Bei, M., Maas, R. and McMahon, A. P. (2000). Sonic hedgehog regulates growth and morphogenesis of the tooth. *Development* **127**, 4775-4785.

Davenport, J. R., Watts, A. J., Roper, V. C., Croyle, M. J., van Groen, T., Wyss, J. M., Nagy, T. R., Kesterson, R. A. and Yoder, B. K. (2007). Disruption of intraflagellar transport in adult mice leads to obesity and slow-onset cystic kidney disease. *Curr. Biol.* **17**, 1586-1594.

Elofsson, R., Andersson, A., Falck, B. and Sjoborg, S. (1984). The ciliated human keratinocyte. *J. Ultrastruct. Res.* **87**, 212-220.

Fischer, E., Legue, E., Doyen, A., Nato, F., Nicolas, J. F., Torres, V., Yaniv, M. and Pontoglio, M. (2006). Defective planar cell polarity in polycystic kidney disease. *Nat. Genet.* **38**, 21-23.

Fuchs, E. (2007). Scratching the surface of skin development. *Nature* **445**, 834-842.

Fuchs, E. (2009). Finding one's niche in the skin. *Cell Stem Cell* **4**, 499-502.

Gerdes, J. M., Liu, Y., Zaghloul, N. A., Leitch, C. C., Lawson, S. S., Kato, M., Beachy, P. A., Beales, P. L., DeMartino, G. N., Fisher, S. et al. (2007). Disruption of the basal body compromises proteasomal function and perturbs intracellular Wnt response. *Nat. Genet.* **39**, 1350-1360.

Goetz, S. C. and Anderson, K. V. (2010). The primary cilium: a signalling centre during vertebrate development. *Nat. Rev. Genet.* **11**, 331-344.

Grachtchouk, V., Grachtchouk, M., Lowe, L., Johnson, T., Wei, L., Wang, A., de Sauvage, F. and Dlugosz, A. A. (2003). The magnitude of hedgehog signaling activity defines skin tumor phenotype. *EMBO J.* **22**, 2741-2751.

Gritli-Linde, A., Hallberg, K., Harfe, B. D., Reyahi, A., Kannius-Janson, M., Nilsson, J., Cobourne, M. T., Sharpe, P. T., McMahon, A. P. and Linde, A. (2007). Abnormal hair development and apparent follicular transformation to mammary gland in the absence of hedgehog signaling. *Dev. Cell* **12**, 99-112.

Gu, L. H. and Coulombe, P. A. (2008). Hedgehog signaling, keratin 6 induction, and sebaceous gland morphogenesis: implications for pachyonychia congenita and related conditions. *Am. J. Pathol.* **173**, 752-761.

Hamamoto, N., Ashizawa, N., Niigaki, M., Kaji, T., Katsube, T., Endoh, H., Watanabe, M., Sumi, S. and Kinoshita, Y. (2002). Morphological changes in the rat exocrine pancreas after pancreatic duct ligation. *Histol. Histopathol.* **17**, 1033-1041.

Harfe, B. D., Scherz, P. J., Nissim, S., Tian, H., McMahon, A. P. and Tabin, C. J. (2004). Evidence for an expansion-based temporal Shh gradient in specifying vertebrate digit identities. *Cell* **118**, 517-528.

Haycraft, C. J., Banizs, B., Aydin-Son, Y., Zhang, Q., Michaud, E. J. and Yoder, B. K. (2005). Gli2 and gli3 localize to cilia and require the intraflagellar transport protein polaris for processing and function. *PLoS Genet.* **1**, e53.

Haycraft, C. J., Zhang, Q., Song, B., Jackson, W. S., Detloff, P. J., Serra, R. and Yoder, B. K. (2007). Intraflagellar transport is essential for endochondral bone formation. *Development* **134**, 307-316.

Hellman, N. E., Liu, Y., Merkel, E., Austin, C., Le Corre, S., Beier, D. R., Sun, Z., Sharma, N., Yoder, B. K. and Drummond, I. A. (2010). The zebrafish foxj1a transcription factor regulates cilia function in response to injury and epithelial stretch. *Proc. Natl. Acad. Sci. USA* **107**, 18499-18504.

Hoseong Yang, S., Andl, T., Grachtchouk, V., Wang, A., Liu, J., Syu, L. J., Ferris, J., Wang, T. S., Glick, A. B., Millar, S. E. et al. (2008). Pathological responses to oncogenic Hedgehog signaling in skin are dependent on canonical Wnt/beta-catenin signaling. *Nat. Genet.* **40**, 1130-1135.

Huangfu, D. and Anderson, K. V. (2005). Cilia and Hedgehog responsiveness in the mouse. *Proc. Natl. Acad. Sci. USA* **102**, 11325-11330.

Huangfu, D., Liu, A., Rakeman, A. S., Murcia, N. S., Niswander, L. and Anderson, K. V. (2003). Hedgehog signalling in the mouse requires intraflagellar transport proteins. *Nature* **426**, 83-87.

Ichikawa, T., Suenaga, Y., Koda, T., Ozaki, T. and Nakagawara, A. (2008). DeltaNp63/BMP-7-dependent expression of matrilin-2 is involved in keratinocyte migration in response to wounding. *Biochem. Biophys. Res. Commun.* **369**, 994-1000.

Ito, M., Liu, Y., Yang, Z., Nguyen, J., Liang, F., Morris, R. J. and Cotsarelis, G. (2005). Stem cells in the hair follicle bulge contribute to wound repair but not to homeostasis of the epidermis. *Nat. Med.* **11**, 1351-1354.

Jonassen, J. A., San Agustin, J., Follit, J. A. and Pazour, G. J. (2008). Deletion of IFT20 in the mouse kidney causes misorientation of the mitotic spindle and cystic kidney disease. *J. Cell Biol.* **183**, 377-384.

Jonkers, J., Meuwissen, R., van der Gulden, H., Peterse, H., van der Valk, M. and Berns, A. (2001). Synergistic tumor suppressor activity of BRCA2 and p53 in a conditional mouse model for breast cancer. *Nat. Genet.* **29**, 418-425.

Koster, M. I., Kim, S., Mills, A. A., DeMayo, F. J. and Roop, D. R. (2004). p63 is the molecular switch for initiation of an epithelial stratification program. *Genes Dev.* **18**, 126-131.

Lechler, T. and Fuchs, E. (2005). Asymmetric cell divisions promote stratification and differentiation of mammalian skin. *Nature* **437**, 275-280.

Lehman, J. M., Michaud, E. J., Schoeb, T. R., Aydin-Son, Y., Miller, M. and Yoder, B. K. (2008). The Oak Ridge Polycystic Kidney mouse: modeling ciliopathies of mice and men. *Dev. Dyn.* **237**, 1960-1971.
Lehman, J. M., Laag, E., Michaud, E. J. and Yoder, B. K. (2009). An essential role for dermal primary cilia in hair follicle morphogenesis. *J. Invest. Dermatol.* **129**, 438-448.
Levy, V., Lindon, C., Harfe, B. D. and Morgan, B. A. (2005). Distinct stem cell populations regenerate the follicle and interfollicular epidermis. *Dev. Cell* **9**, 855-861.
Levy, V., Lindon, C., Zheng, Y., Harfe, B. D. and Morgan, B. A. (2007). Epidermal stem cells arise from the hair follicle after wounding. *FASEB J.* **21**, 1358-1366.
Liu, A., Wang, B. and Niswander, L. A. (2005). Mouse intraflagellar transport proteins regulate both the activator and repressor functions of Gli transcription factors. *Development* **132**, 3103-3111.
Marszalek, J. R., Liu, X., Roberts, E. A., Chui, D., Marth, J. D., Williams, D. S. and Goldstein, L. S. (2000). Genetic evidence for selective transport of opsin and arrestin by kinesin-II in mammalian photoreceptors. *Cell* **102**, 175-187.
May, S. R., Ashique, A. M., Karlen, M., Wang, B., Shen, Y., Zarbalis, K., Reiter, J., Ericson, J. and Peterson, A. S. (2005). Loss of the retrograde motor for IFT disrupts localization of Smo to cilia and prevents the expression of both activator and repressor functions of Gli. *Dev. Biol.* **287**, 378-389.
Mill, P., Mo, R., Fu, H., Grachtchouk, M., Kim, P. C., Dlugosz, A. A. and Hui, C. C. (2003). Sonic hedgehog-dependent activation of Gli2 is essential for embryonic hair follicle development. *Genes Dev.* **17**, 282-294.
Mills, A. A., Zheng, B., Wang, X. J., Vogel, H., Roop, D. R. and Bradley, A. (1999). p63 is a p53 homologue required for limb and epidermal morphogenesis. *Nature* **398**, 708-713.
Morris, R. J. and Potten, C. S. (1999). Highly persistent label-retaining cells in the hair follicles of mice and their fate following induction of anagen. *J. Invest. Dermatol.* **112**, 470-475.
Nieuwenhuis, E., Motoyama, J., Barnfield, P. C., Yoshikawa, Y., Zhang, X., Mo, R., Crackower, M. A. and Hui, C. C. (2006). Mice with a targeted mutation of patched2 are viable but develop alopecia and epidermal hyperplasia. *Mol. Cell. Biol.* **26**, 6609-6622.
Nieuwenhuis, E., Barnfield, P. C., Makino, S. and Hui, C. C. (2007). Epidermal hyperplasia and expansion of the interfollicular stem cell compartment in mutant mice with a C-terminal truncation of Patched1. *Dev. Biol.* **308**, 547-560.
Panteleyev, A. A., Paus, R., Wanner, R., Nurnberg, W., Eichmuller, S., Thiel, R., Zhang, J., Henz, B. M. and Rosenbach, T. (1997). Keratin 17 gene expression during the murine hair cycle. *J. Invest. Dermatol.* **108**, 324-329.
Patel, V., Li, L., Cobo-Stark, P., Shao, X., Somlo, S., Lin, F. and Igarashi, P. (2008). Acute kidney injury and aberrant planar cell polarity induce cyst formation in mice lacking renal cilia. *Hum. Mol. Genet.* **17**, 1578-1590.
Piontek, K., Menezes, L. F., Garcia-Gonzalez, M. A., Huso, D. L. and Germino, G. G. (2007). A critical developmental switch defines the kinetics of kidney cyst formation after loss of Pkd1. *Nat. Med.* **13**, 1490-1495.
Potten, C. S. and Morris, R. J. (1988). Epithelial stem cells in vivo. *J. Cell Sci. Suppl.* **10**, 45-62.
Ro, S. and Rannala, B. (2005). Evidence from the stop-EGFP mouse supports a niche-sharing model of epidermal proliferative units. *Exp. Dermatol.* **14**, 838-843.
Romano, R. A., Birkaya, B. and Sinha, S. (2007). A functional enhancer of keratin14 is a direct transcriptional target of deltaNp63. *J. Invest. Dermatol.* **127**, 1175-1186.
Romano, R. A., Ortt, K., Birkaya, B., Smalley, K. and Sinha, S. (2009). An active role of the DeltaN isoform of p63 in regulating basal keratin genes K5 and K14 and directing epidermal cell fate. *PLoS One* **4**, e5623.
Romano, R. A., Smalley, K., Liu, S. and Sinha, S. (2010). Abnormal hair follicle development and altered cell fate of follicular keratinocytes in transgenic mice expressing DeltaNp63alpha. *Development* **137**, 1431-1439.
Schneider, M. R., Schmidt-Ullrich, R. and Paus, R. (2009). The hair follicle as a dynamic miniorgan. *Curr. Biol.* **19**, R132-R142.
Sharma, N., Berbari, N. F. and Yoder, B. K. (2008). Ciliary dysfunction in developmental abnormalities and diseases. *Curr. Top. Dev. Biol.* **85**, 371-427.
St-Jacques, B., Dassule, H. R., Karavanova, I., Botchkarev, V. A., Li, J., Danielian, P. S., McMahon, J. A., Lewis, P. M., Paus, R. and McMahon, A. P. (1998). Sonic hedgehog signaling is essential for hair development. *Curr. Biol.* **8**, 1058-1068.
Taulman, P. D., Haycraft, C. J., Balkovetz, D. F. and Yoder, B. K. (2001). Polaris, a protein involved in left-right axis patterning, localizes to basal bodies and cilia. *Mol. Biol. Cell* **12**, 589-599.
Tumbar, T., Guasch, G., Greco, V., Blanpain, C., Lowry, W. E., Rendl, M. and Fuchs, E. (2004). Defining the epithelial stem cell niche in skin. *Science* **303**, 359-363.
Vasioukhin, V., Degenstein, L., Wise, B. and Fuchs, E. (1999). The magical touch: genome targeting in epidermal stem cells induced by tamoxifen application to mouse skin. *Proc. Natl. Acad. Sci. USA* **96**, 8551-8556.
Verghese, E., Weidenfeld, R., Bertram, J. F., Ricardo, S. D. and Deane, J. A. (2008). Renal cilia display length alterations following tubular injury and are present early in epithelial repair. *Nephrol. Dial. Transplant.* **23**, 834-841.
Verghese, E., Ricardo, S. D., Weidenfeld, R., Zhuang, J., Hill, P. A., Langham, R. G. and Deane, J. A. (2009). Renal primary cilia lengthen after acute tubular necrosis. *J. Am. Soc. Nephrol.* **20**, 2147-2153.
Wandel, A., Steigleder, G. K. and Bodeux, E. (1984). Primary cilia in cells of the epidermis and dermis. *Z. Hautkr.* **59**, 389-392.
Wang, L., Weidenfeld, R., Verghese, E., Ricardo, S. D. and Deane, J. A. (2008). Alterations in renal cilium length during transient complete ureteral obstruction in the mouse. *J. Anat.* **213**, 79-85.
Warfvinge, K. and Elofsson, R. (1988). Single modified cilia displayed by cells of human internal stratified epithelia (oral cavity, vagina). *Cell Tissue Res.* **251**, 237-241.
Watt, F. M. and Jensen, K. B. (2009). Epidermal stem cell diversity and quiescence. *EMBO Mol. Med.* **1**, 260-267.
Wong, S. Y., Seol, A. D., So, P. L., Ermilov, A. N., Bichakjian, C. K., Epstein, E. H., Jr, Dlugosz, A. A. and Reiter, J. F. (2009). Primary cilia can both mediate and suppress Hedgehog pathway-dependent tumorigenesis. *Nat. Med.* **15**, 1055-1061.
Xie, J., Murone, M., Luoh, S. M., Ryan, A., Gu, Q., Zhang, C., Bonifas, J. M., Lam, C. W., Hynes, M., Goddard, A. et al. (1998). Activating Smoothened mutations in sporadic basal-cell carcinoma. *Nature* **391**, 90-92.
Yang, A., Schweitzer, R., Sun, D., Kaghad, M., Walker, N., Bronson, R. T., Tabin, C., Sharpe, A., Caput, D., Crum, C. et al. (1999). p63 is essential for regenerative proliferation in limb, craniofacial and epithelial development. *Nature* **398**, 714-718.